Carbon Nanotubes Generated from Template Carbonization of Polyphenyl Acetylene as the Support for Electrooxidation of Methanol

B. Rajesh,[†] K. Ravindranathan Thampi,*[,‡] J.-M. Bonard,[§] N. Xanthopoulos,[||] H. J. Mathieu,[||] and B. Viswanathan*[,†]

Department of Chemistry, Indian Institute of Technology, Madras, Chennai-600036, India, Laboratory of Photonics and Interfaces, ICMB-LPI, Swiss Federal Institute of Technology, Lausanne CH-1015, Switzerland, Group de Physique des aggregate en surface, FSB, Swiss Federal Institute of Technology, Lausanne, CH-1015, Switzerland, and Laboratoire de Metallurgie Chimique, Swiss Federal Institute of Technology, Lausanne, CH-1015, Switzerland

Received: August 21, 2002; In Final Form: December 1, 2002

The template carbonization of polyphenyl acetylene yielded well aligned, cylindrical, mono disperse carbon nanotubes (CNT), which are effectively utilized to load Pt, Pt−Ru, and Pt−WO_3 nano particles. The nanoparticles are effectively dispersed inside the tube with the particle sizes of around 1.2, 1.6, and 10 nm for Pt, Pt−Ru, and Pt−WO_3, respectively. The electrochemical surface area of the CNT-based electrode was higher compared to the Vulcun XC 72R carbon, graphite, and glassy carbon (GC) electrodes. The X-ray photoelectron spectroscopic measurements revealed that the Pt and Ru are in metallic state and W is in +VI oxidation state. The higher activity of GC/CNT−Pt−WO_3−Nafion for methanol oxidation compared to GC/CNT/Pt−Ru−Nafion and GC/CNT/Pt−Nafion suggests the better utilization of the catalytic particles. The stability of the electrode for methanol oxidation polarized at +0.6 V follows the order of GC/CNT/Pt−Ru−Nafion > GC/CNT/Pt−WO_3 > GC/CNT/Pt−Nafion, and for the electrodes polarized at +0.4 V, the order is GC/CNT/Pt−WO_3−Nafion > GC/CNT/Pt−Ru−Nafion > GC/CNT/Pt−Nafion. The differences in the stability possibly suggest the better tolerance of the adsorbed species of methanol oxidation for the GC/CNT/Pt−WO_3−Nafion electrode (when it is polarized at +0.4 V).

1. Introduction

The tubular structure of carbon nanotubes makes them unique among different forms of carbon, and they can thus be exploited as an alternative material for catalyst support in heterogeneous catalysis[1] and in fuel cells.[2,3] The discovery of the carbon nanotube (CNT) was based on the carbon-arc method,[4] and the carbon nanotubes prepared by this method are more graphitic with low yields, thus making the production cost very high. The template synthesis[5] and catalytic production methods[6] do not have some of these limitations. The normal source of carbon to produce the carbon nanotubes is hydrocarbons.[7,8] It has been reported that the carbonization of carbon sources that contain nitrogen[9] leads to carbon nano or micro tubules containing nitrogen, and the topology of the carbon nanotube formed is altered as a function of the amount of nitrogen in the nanotube.[10] Recently, we reported the synthesis of the carbon nanotubes by the template carbonization of polypyrrole[11] (a source which contains nitrogen) and polyphenyl acetylene[12] as the carbon source, where only carbon−hydrogen bonds have to be broken during the thermal treatment, so it can be an ideal starting material for the preparation of the carbon nanotubes.

Considerable interest has been developed in recent years[13−18] to develop suitable electrode materials for methanol oxidation for the possible application in direct methanol fuel cells (DMFC). Currently, Pt−Ru particles supported on carbon is the most promising catalyst material for anode in DMFC. The superior activity of Pt−Ru/C over Pt/C is due to the improved CO tolerance of the alloy. Significant progress has been made to reduce the loading level of Pt and to increase the stability of the electrode for methanol oxidation. In that process, Pt−WO_3[19−21] and Pt−MoO_3[22] catalysts have been evaluated as electrodes. Though these catalysts exhibit higher peroformance and stability than pure Pt, the activity of methanol oxidation is still not high enough to be put into commercial applications. The probable reason for this could be due to the poor utilization of the catalyst, which is due to the larger particle size (150−200 nm), which forms agglomerates. It has been speculated that because of the unique properties of the CNT, this material can be used as the support for the catalytic particles. Pt supported on graphite nanofibers has been reported for methanol oxidation, and the observed activity has also been compared with Pt supported on Vulcan XC 72 carbon. It has been shown[23] that the Pt supported on graphite nanofibers not only exhibited higher activity but also showed better stability. We have recently reported[24,25] the results of the study on Pt−WO_3, Pt−Ru, and Pt supported on the carbon nanotube generated from the template carbonization of polypyrrole for electro-oxidation of methanol. We also showed the effect of nitrogen content on the catalytic activity of the electrodes. In the present investigation, we used a similar method to load Pt−WO_3, Pt−Ru, and Pt on the carbon nanotube generated from the polyphenyl acetylene.

* Authors to whom correspondence should be addressed. E-Mail: Ravindranathan.Thampi@epfl.ch; bviswanathan@hotmail.com.

[†] Indian Institute of Technology.

[‡] Laboratory of Photonics and Interfaces, Swiss Federal Institute of Technology.

[§] Group de Physique des aggregate en surface, Swiss Federal Institute of Technology.

[||] Laboratoire de Metallurgie Chimique, Swiss Federal Institute of Technology.

10.1021/jp0219350 CCC: $25.00
Published on Web 03/04/2003

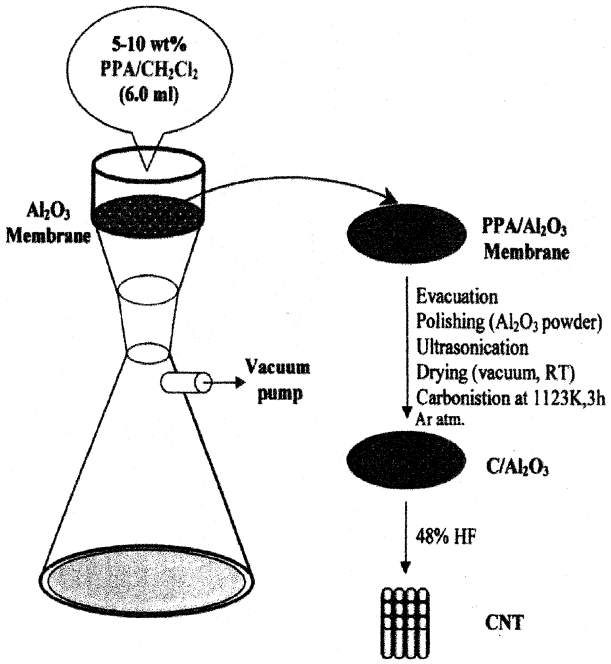

Figure 1. The pictorial representation of synthesis of carbon nanotubes based on carbonization of polyhenyl acetylene).

SCHEME 1: Schematic Representation of Synthesis of WO_3 and Pt−WO_3 Loaded Carbon Nanotube by Carbonization of Polyphenyl Acetylene Using Alumina Membrane as Template

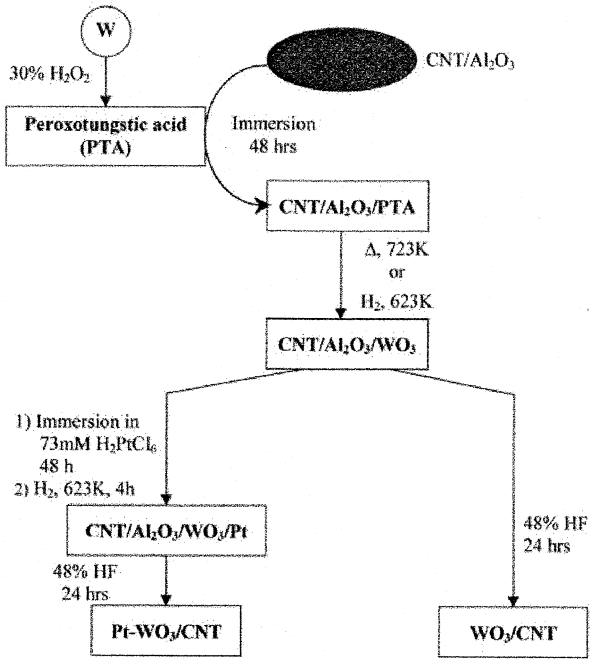

2. Experimental Section

2.1. Materials. All the chemicals used were of analytical grade. Phenyl acetylene and $W(CO)_6$ were purchased from Fluka. Hydrofluoric acid, methanol, sulfuric acid, tungsten metal powder, and hydrogen peroxide (30%) (all from Merck) were used as received. Hexa-chloro-platinic acid and ruthenium chloride were obtained from Hindustan Platinum Ltd. Nafion 5% solution (from Aldrich) was used as received. Alumina template membranes (0.2 μm pore diameter and 60 μm thick) were obtained commercially (Whatman Anopore Filters, Altech). Glassy carbon was polished with fine alumina powder and was ultrasonicated in water prior to use. 20% Pt/Vulcan Carbon Pt−Ru/Vulcan carbon catalysts were obtained from E-Tek.

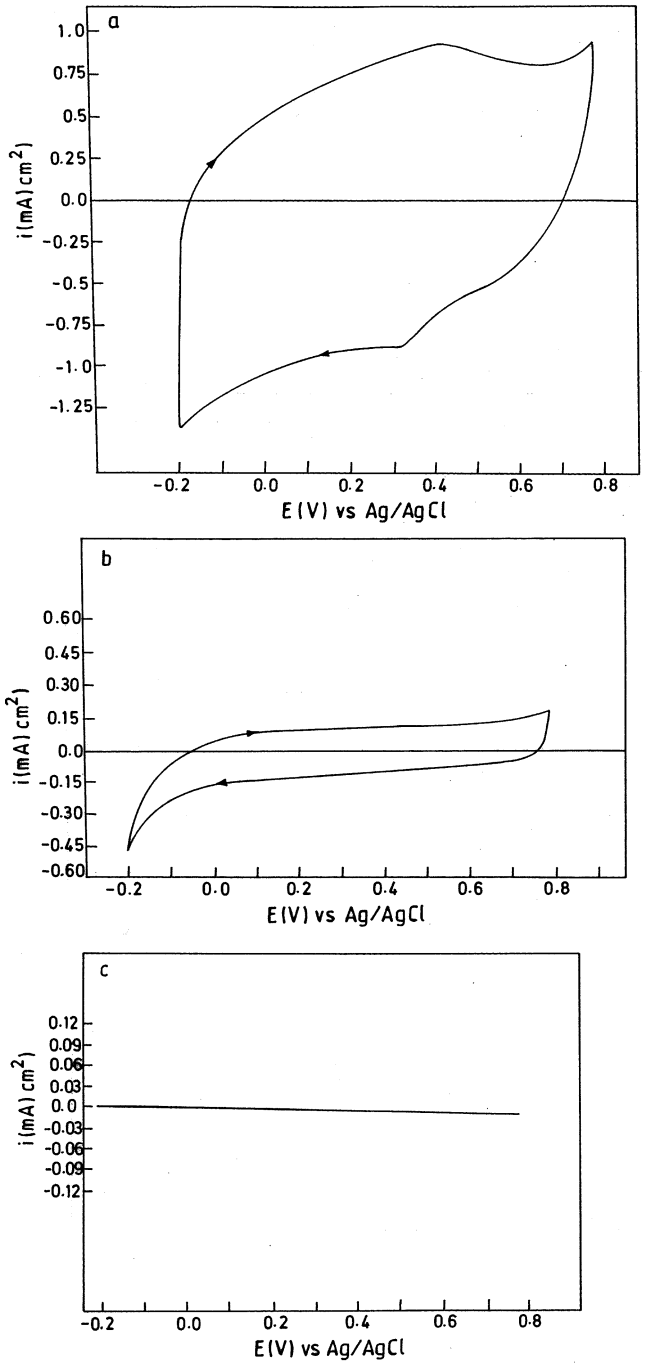

Figure 2. Cyclic voltammetric response of (a) the GC/CNT-Naf and (b) GC/Vulcan XC 72 carbon−Naf (c) GC electrodes in 1 M H_2SO_4 at 50 mV/s between −0.2 V and +0.8 V vs Ag/AgCl.

2.2. Characterization Methods. Scanning electron microscopic images were obtained using a JEOL 1500 microscope. The carbon nanotubes obtained after the dissolution of the template were immersed in ethanol and ultrasonicated for 20 min to disperse them completely. A drop of this suspension was placed on an SEM sample holder, sputter coated with gold to prevent charging, and then imaged. The microscopic features of the samples were also observed with high-resolution transmission electron microscope (HR-TEM, Philips EM430ST) operated at 300 kV. The samples were dispersed in ethanol under sonication, dropped on the carbon coated TEM grids, and then

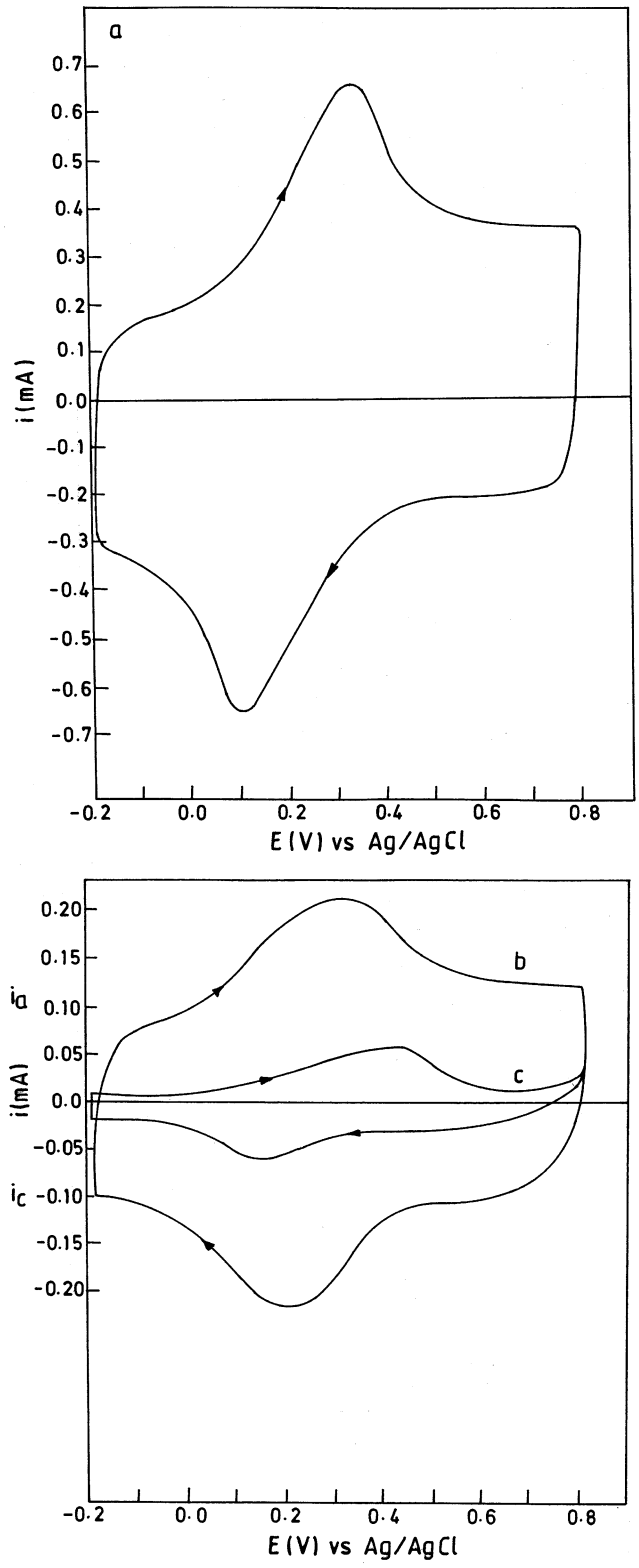

Figure 3. Cyclic voltammograms of (a) GC/CNT−Nafion (b) GC/Vulcan XC 72−carbon−Naf and (c) GC electrodes in 5 mM $K_4[Fe(CN)_6]$/0.1 M KCl run at 50 mV/s between −0.2 and +0.8 V vs Ag/AgCl.

imaged. The X-ray photoelectron spectroscopic (XPS) measurements of nanoparticles loaded carbon nanotubes were carried out with a Perkin−Elmer PHI 5500 ESCA system using Mg K α as excitation source. The bulk Pt on the catalyst/electrode was analyzed by an inductively coupled plasma atomic emission spectrometer (ICPAES, model 3410, ARL) after calibration with standard solution containing a known metal content. The metal was extracted from the catalyst/electrode by boiling in aqua regia.

2.3. Synthesis of Carbon Nanotubes. The polyphenyl acetylene was prepared by photoinitiation of phenylacetylene[26] by $W(CO)_6$ (Fluka). The polyphenyl acetylene/alumina composite was prepared by adding 10 mL of 5% w/w polyphenyl acetylene (in dichloro methane) to the alumina membrane (Whatman, 200 nm pore diameter, 60μm thick, 17.34 cm^2) and applying vacuum from the bottom. The entire polymer solution penetrates inside the pores of the membrane by the suction applied. The solvent was evaporated slowly, and the membrane was dried in a vacuum at 373 K. for 10 min. The composite was then polished with fine alumina powder to remove the surface layers and ultrasonicated for 20 min to remove the residual alumina used for polishing. The composite was then carbonized by heating in Ar atmosphere at different temperatures between 1023 and 1173 K, and the time was varied between 2 and 4 h at a heating rate of 10 °C/min. This resulted in the deposition of carbon on the channel walls of the membrane. The carbon/alumina composite was then placed in 48% HF to free the nanotubules. The tubules left behind in HF were completely washed with deionized water to remove HF. The pictorial representation of the synthetic procedure is shown in Figure 1.

2.4. Loading of Metal(s) Nanocluster Inside CNTs. Pt or Pt−Ru nanoclusters were loaded inside the CNT as follows: The C/alumina composite obtained (before the dissolution of template membrane) was immersed in 73 mM H_2PtCl_6(aq) or in a mixture of 37 mM hexachloroplatinic acid and 73 mM ruthenium chloride for 12 h. After immersion, the membrane was dried in air, and the ions were reduced to the corresponding metal(s) by a 3 h exposure to flowing H_2 gas at 823 K. The underlying alumina was then dissolved by immersing the composite in 48% HF for 24 h. The membrane was removed from the HF solution and treated in the same way as for unloaded CNT to remove residual HF. These processes resulted in Pt or Pt−Ru nanocluster loaded CNT.

2.5. Loading of WO_3 and Pt−WO_3 Inside Carbon Nanotubes. The carbon/alumina composite was immersed in peroxotungstic acid solution (obtained by dissolving W metal powder in 30% H_2O_2, followed by the decomposition of excess H_2O_2 using platinized platinum, and the concentration of peroxotungstic acid with respect to W was 0.1 M) for between 24 and 48 h. The material was ultrasonicated for 5 min to remove any precipitate that was formed on the composite (polymeric form of tungsten oxides may be precipitated upon prolonged standing). The immersion leads to the penetration of peroxo tungstic acid inside the pores of the composite. The composite was then dried in air at room temperature for 1 h and heated at 723 K for 4 h, which resulted in the formation of WO_3. The WO_3 incorporated carbon nanotube (WO_3/CNT) was collected by dissolving the template (alumina membrane) in 48% HF for 24 h. The residue was completely washed with deionized water several times to remove the HF.

The WO_3/carbon/alumina composite was immersed in 73 mM H_2PtCl_6 for 48 h, dried, and reduced at 623 K for 4 h in H_2 atmosphere. The alumina membrane was dissolved in 48% HF for 24 h. It was then repeatedly washed with deionized water to remove HF and dried in air at 333 K to obtain Pt/WO_3 incorporated CNTs. The sequence of loading of WO_3/Pt−WO_3 is depicted in Scheme 1.

2.6. Preparation of Composite Electrodes. The electrodes for the electrochemical measurements were fabricated by

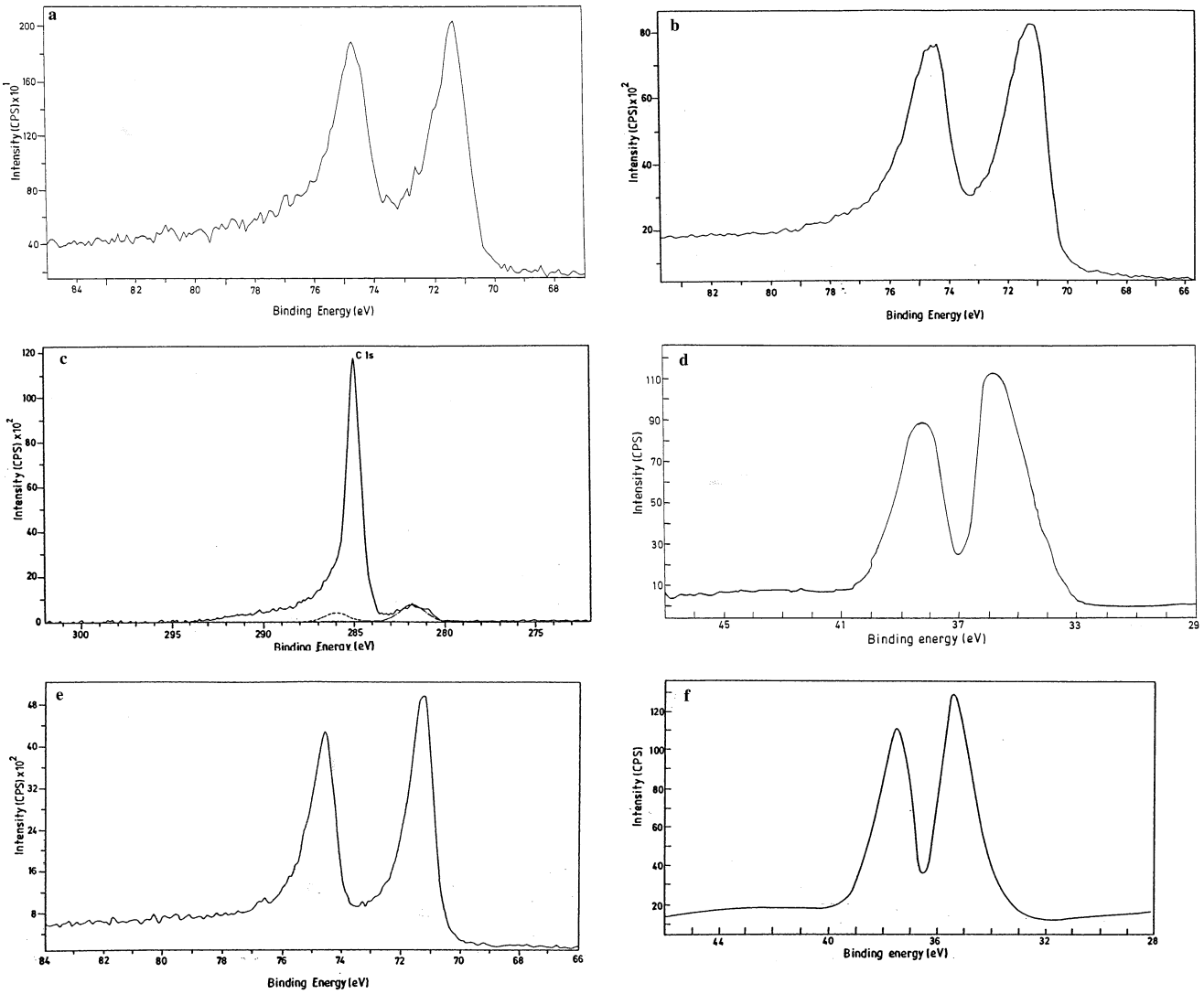

Figure 4. (a) X-ray photoelectron spectra of Pt 4f in Pt loaded CNT. X-ray photoelectron spectra of (b) Pt 4f in Pt−Ru loaded CNT and (c) Ru 3d in Pt−Ru loaded CNT (also shown *C1s* of Pt−Ru loaded CNT in (c)). (d) X-ray photoelectron spectra of W 4f in WO_3 loaded CNT. X-ray photoelectron spectra of (e) Pt 4f in Pt−WO_3 loaded CNT and (f) W 4f in Pt−WO_3 loaded CNT.

dispersing the unloaded or loaded CNT (after the template removal) in 200 μL of deionized water, to which 25 μL of 5 wt % Nafion solution was then added, and the dispersion was then ultrasonicated for 20 min. A known amount of suspension was added on to the glassy carbon (GC) electrode, and the solvent was slowly evaporated, which results in an unloaded or loaded GC/CNT−Nafion composite electrode.

2.7. Electrocatalytic Measurements. Electrocatalytic measurements were made with a Wenking potentio scan (POS73) with digital 2000 X−Y recorder. A three electrode cell consisting of the glassy carbon (0.07 cm^2) working electrode, Pt foil (1 cm^2) counter electrode, and Ag/AgCl reference electrode was used for studies. The electrochemical experiments were performed in sulfuric acid medium in the presence and absence of methanol. The stability of the electrodes was evaluated from current−time plot by polarizing the electrode at particular potential with respect to time in 1M H_2SO_4 and 1 M CH_3OH.

3. Results and Discussion

3.1. Electron Microscopy Study. The HR-TEM (figure not shown) after the carbonization at 1173 K for 4 h shows hollow tubes with slight deformation in the end of the tube, probably caused by the ultrasonication and vigorous HF treatment. Micrograph also indicates the formation of a cylindrical, monodisperse tube, which is hollow and transparent, indicating that the wall of the tube is thin and the open end of the tube can be utilized to load the particles. The outer diameter of the tube is almost 200 nm, which corresponds to the channel diameter of the template used (also seen is a layer of amorphous carbon on the wall of the tube). Though the carbon tubes produced by this method are not completely graphitic in nature, as those produced by arc-discharge process are, their disordered structure is quite typical of fibers or nanotubes produced by decomposition of hydrocarbons, as is evident from the amorphous carbon on the wall of the carbon nanotube.

The HR-TEM of Pt, Pt−Ru, and Pt−WO_3 loaded nanotubes reveals that the particles are highly dispersed inside the nanotube, with average particle sizes of 1.2 nm for Pt, 3 nm for Pt−Ru, and 10 nm for Pt−WO_3. This also demonstrates that the open end of the tube has been effectively utilized to load the particles.

3.2. Electrochemical Behavior of GC/CNT−Nafion Electrode in 1 M H_2SO_4. Figure 2a shows the cyclic voltammogram of CNT−Nafion coated GC in 1 M H_2SO_4 scanned between −0.2 V and +0.8 V vs Ag/AgCl at a scan rate of 50 mV/s,

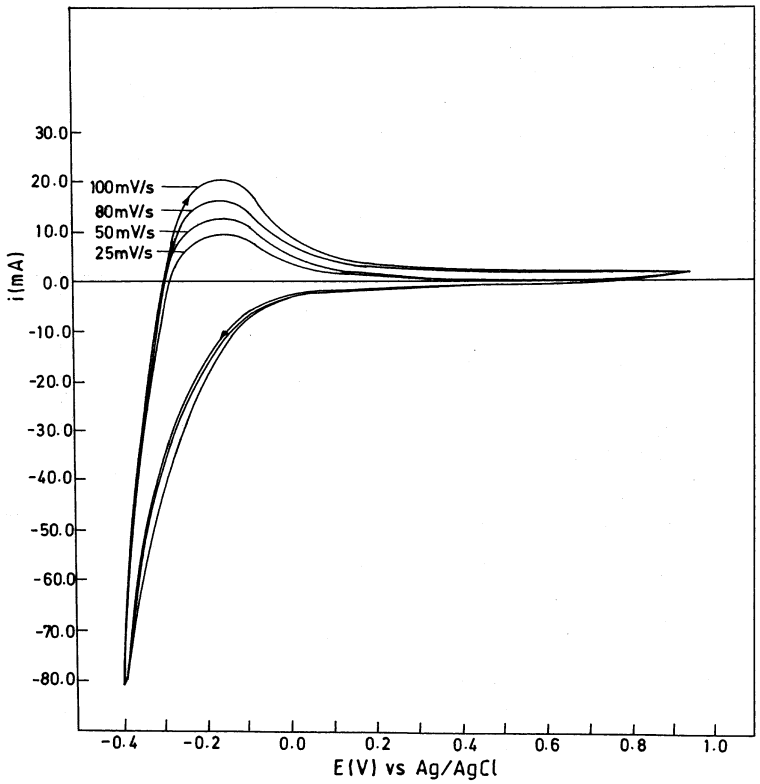

Figure 5. Cyclic voltammetric response of the GC/CNT−WO_3−Nafion electrode in 1 M H_2SO_4 at 25, 50, 80, and 100 mV/s between −0.4 and +0.8 V vs Ag/AgCl.

with the corresponding voltammograms obtained for Vulcan XC 72 R carbon (Figure 2b) and GC (Figure 2c) electrodes. It is clear from the voltammogram that the GC/CNT-Nafion electrode shows higher background current response[2] for the oxidation and reduction peaks, at +0.42 V and +0.3 V in the forward and reverse scans, respectively, compared to all the other electrodes. This reflects the higher electroactive area available for the carbon-nanotube-based composite electrode, and the observed surface electrochemistry of this material is typical of carbon electrodes.[27]

3.3. Evaluation of Electroactive Surface Area of Electrode Materials. To account for the higher current response, the electroactive surface area of the electrode materials was evaluated from the cyclic voltammagram. The voltammagram was run in 5 mM $K_4[Fe(CN)_6]$ (probe molecule) in 0.1 M KCl at a scan rate of 50 mV/s. The typical voltammogram obtained with the GC/CNT−Nafion electrode is shown in Figure 3a, with the corresponding voltammograms obtained for Vulcan carbon and GC electrodes in Figure 3, parts b and c. The well-defined peak obtained at +0.35 and +0.11 V in the forward and reverse scans is due to the Fe^{3+}/Fe^{2+} redox couple on the GC/CNT−Nafion electrode. The electrochemical surface area has been evaluated from the peak current by using the value of diffusion coefficient of $K_4[Fe(CN)_6]$ as 0.76×10^{-5}cm^2/s in the Randel Sevcik equation ($I_p = 2.69 \times 10^5 A D^{1/2} n^{3/2} \gamma^{1/2} C$).[28] The electroactive surface area was found to be 0.28 cm^2 for the GC/CNT−Nafion electrode, 0.08 cm^2 for Vulcan carbon, and 0.01 cm^2 for glassy carbon electrodes.

3.4. Surface Characterization of Loaded Carbon Nanotubes by XPS. The XPS (Figure 4a) of Pt 4f with peak binding energy of 71.2 eV ($4f_{7/2}$) and 74.8 eV ($4f_{5/2}$) suggest that the Pt particles are present in the metallic state. The peak binding energies of Pt $4f_{7/2}$ at 71.1 eV and Pt $4f_{5/2}$ at 74.5 eV show that the Pt ions are completely reduced (Figure 4b) in the Pt−Ru loaded carbon nanotube. Although the Ru 3d signal is obscured by *C*1*s* signal at 284.5 eV (Figure 4c), the deconvoluted spectra show the doublet with peak binding energies of Ru $3d_{5/2}$ at 280.3 eV and Ru $3d_{3/2}$ at 283.0 eV, and this suggests that the Ru particles are also in the zerovalent state. The XPS of W 4f in WO_3 loaded carbon nanotubes are shown in Figure 4d. The doublet with peak binding energies centered at 35.5 eV of W($4f_{7/2}$) and 37.4 eV of W $4f_{5/2}$ suggests that W is in the +VI oxidation state. Similarly, the peak with binding energies of Pt 4f centered at 71.1 eV of Pt $4f_{7/2}$ and 74.5 eV of Pt $4f_{5/2}$ (Figure 4e) revealed that the Pt is in the zerovalent state in the Pt−WO_3 loaded carbon nanotube. The X-ray photo electron spectra of W (Figure 4f) in Pt−WO_3 shows a doublet with peak binding energies centered at 35.2 eV of W ($4f_{7/2}$) and 37.5 eV of W ($4f_{5/2}$), suggesting that W may be in the +VI oxidation state.

3.5. Electrochemical Behavior of WO_3 Loaded CNTs. The cyclic voltammogram of GC/CNT−WO_3−Nafion electrode run in 1 M H_2SO_4 at different scan rates (25, 50, 80 and 100 mV/s) is shown in Figure 5: The potential was scanned between −0.4 and +0.74 V vs Ag/AgCl. The elctrochemical response due to W is seen at −0.1 V in the forward scan, which clearly matches with the peak reported in the literature.[29]

3.6. Evaluation of Methanol Electrooxidation Activity of Composite Materials. The cyclic voltammogram of GC/CNT−Pt−WO_3−Nafion electrode in 1 M H_2SO_4 (in the absence of methanol) scanned between −0.2 V and +0.8 V and run at 50 mV/s is shown in Figure 6a. A broad peak at −0.1 V is due to the overlap of hydrogen adsorption on Pt[18] as well as to the redox process of W.[29] The cyclic voltammogram of Pt−WO_3, Pt−Ru, and Pt-loaded carbon-nanotube based electrodes are shown in Figure 6, parts b−d. The cyclic voltammogram of GC/CNT−Pt−WO_3−Nafion (Figure 6b) shows the onset potential (potential at which the methanol oxidation starts) at 100 mV with the peak current densities of 80.0 mA/cm^2 at 0.54 V in the forward sweep and 67.8 mA/cm^2 at 0.53 V in the reverse sweep. Though there is an initial increase due to methanol

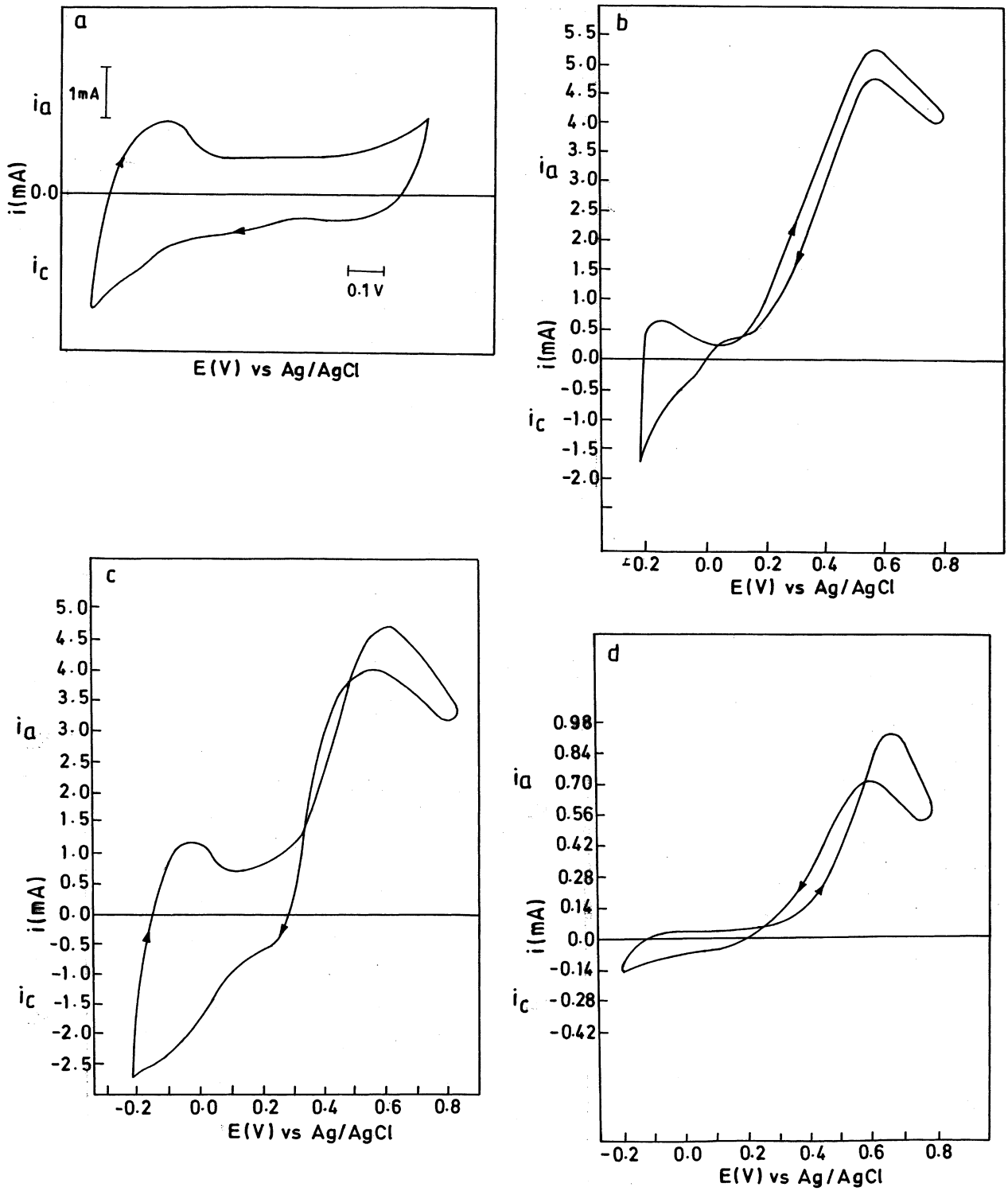

Figure 6. Cyclic voltammograms of (a) the GC/CNT−Pt− WO_3−Nafion electrode in 1 M H_2SO_4 (absence of methanol), (b) the GC/CNT−Pt−WO_3−Nafion, (c) GC/CNT−Pt−Ru−Naf and (d) GC CNT−Pt−Naf electrodes in 1 M H_2SO_4/1 M CH_3OH run at 50 mV/s between −0.2 and +0.8 V vs Ag/AgCl.

oxidation with applied potential up to 0.54 V, the current decreases and reaches 57.1 mA/cm^2 at 0.8 V for GC/CNT−Pt−WO_3−Nafion. However, the difference between the peak potential of only 0.1 V between the forward and the backward sweep possibly indicates the better CO tolerance of the catalyst.[18,19]

The onset of methanol oxidation (Figure 6c) on GC/CNT/Pt−Ru−Nafion electrode was found to be 0.16 V, which is 60 mV more positive than GC/CNT−Pt−WO_3−Nafion electrode. The current increases with the potential and peaks at +0.6 V (which is also 60 mV more positive than the GC/CNT−Pt−WO_3−Nafion electrode), with a current density of 67.1 mA/cm^2 in the forward scan and 58.5 mA/cm^2 at 0.55 V in the reverse scan. The current density in the forward scan at +0.8 V was found to be 46.4 mA/cm^2. Although the peak potential difference (50 mV) was slightly higher than the GC/CNT−Pt−WO_3−Nafion electrode, the magnitude of the current in the reverse scan was close to that obtained in the forward scan,

TABLE 1: Comparison of Electro-Catalytic Activity of Methanol Oxidation on Supported CNT-Based Electrodes

			activity[a]			
			forward sweep		reverse sweep	
S.No	electrode	onset E (V)	I ($mAcm^{-2}$)	E (V)	I ($mAcm^{-2}$)	E (V)
1	GC/CNT/Pt−WO_3	0.10	80.0[b]	0.54	67.8[b]	0.53
			57.4	0.80		
2	GC/CNT/Pt−Ru	0.16	67.1[b]	0.60	58.5[b]	0.55
			46.4	0.80		
3	GC/CNT/Pt	0.20	13.3[b]	0.66	10.0[b]	0.6
			8.3	0.80		

[a] Activity evaluated from cyclic voltammogram run in 1 M H_2SO_4/1 M CH_3OH scanned between −0.2 and +0.8 V vs Ag/AgCl at 50 mV/s. [b] Peak current density (mA/cm^2).

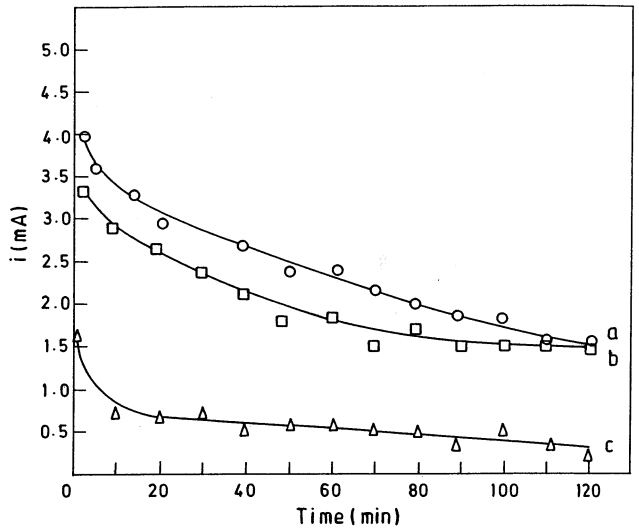

Figure 7. Chronoamperometric response of (a) GC/CNT−Pt−WO_3−Nafion, (b) GC/CNT−Pt−Ru−Nafion, and (c) GC/CNT−Pt−Nafion electrodes polarized at +0.6 V in 1 M H_2SO_4/1 M CH_3OH for 2 h.

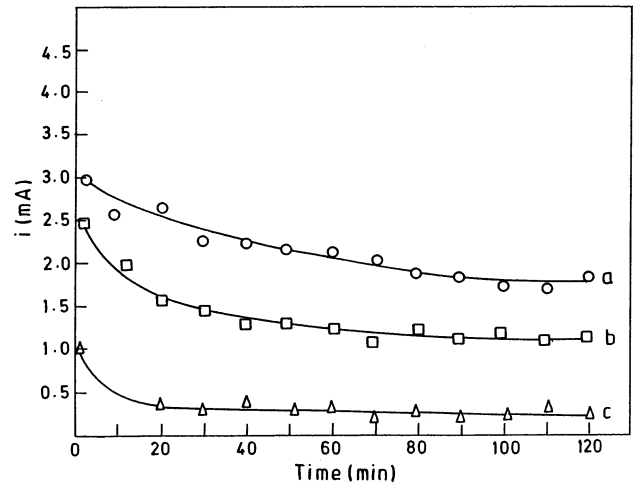

Figure 8. Chronoamperometric response of (a) GC/CNT−Pt−WO_3−Nafion, (b) GC/CNT−Pt−Ru−Nafion, and (c) GC/CNT−Pt−Nafion electrode polarized at +0.4 V in 1 M H_2SO_4/1 M CH_3OH for 2 h.

which suggests that the bifunctional mechanism might play a major role for the observed behavior for both the electrodes. The onset of methanol oxidation on the GC/CNT/−Pt−Nafion electrode (Figure 6d) was 40 mV more positive than the GC/CNT/−Pt−Ru−Nafion electrode and 100 mV more positive than the GC/CNT−Pt−WO_3−Nafion electrode. The maximum activity in the forward scan was found to be 13.3 mA/cm^2 at 0.66 V in the forward scan and 10 mA/cm^2 at 0.6 V in the reverse scan. The current density increase observed after the hydrogen evolution potential window (in the present case it is between −0.2 V and +0.8 V vs Ag/AgCl electrode) is the threshold current density. The value of the threshold current density will vary with the type of electrode and also with Pt loading and its accessibility to the reactants. The poor activity of the Pt loaded nanotube might be due to the very fine dispersion of Pt particles, which resulted in the particles slightly below the critical particle size requirement for the oxidation. The data obtained from the cyclic voltammogram are compiled in Table 1.

The amount of Pt was found to be 24, 39, and 33 μg on GC/CNT−Pt−Naf, GC/CNT−Pt−Ru−Naf and GC/CNT/Pt−WO_3−Naf electrodes, respectively. Because the amount of noble metal, especially Pt, in the fuel cell electrode is mainly responsible for the oxidation of methanol, the inductively coupled plasma analysis was done only for Pt in the present study. The difference in Pt loading might be due to a process step. The uptake of Pt during the loading step and the leaching of Pt during the dissolution of the template would have varied marginally between the samples, which resulted in different Pt loadings.

3.7. Chronoamperometric Response of Composite Electrodes Based on CNT for Methanol Oxidation. *3.7.1. Electrodes Polarized at 0.6 V in 1M H_2SO_4/1M CH_3OH for 2 h.* Figure 7a shows the chronoamperometric response of the GC/CNT−Pt−WO_3−Nafion electrode. It is clear from Figure 7a that in spite of the initial high current density, there is a constant decay in the current with respect to time, possibly suggesting the poisoning of the electrode is due to the faster dissolution of the W from the electrode. On the other hand, for the GC/CNT−Pt−Ru−Nafion electrode (Figure 7b), though there is a gradual decay for a period of 80 min, the current appears to be quite stable afterward, suggesting the better tolerance of the Pt−Ru catalyst. In the case of the GC/CNT/Pt−Nafion electrode (Figure 7c), the decrease was so rapid that it reached the minimum within 20 min.

3.7.2. Electrodes Polarized at 0.4 V in 1M H_2SO_4/1M CH_3OH for 2 h. Figure 8a shows the chronoamperometric response of the GC/CNT−Pt−WO_3−Nafion electrode. It is clear from Figure 8a that the rate of decay of the current was quite low when the electrode was polarized at +0.4 V. The electrode not only showed higher initial activity but also was fairly stable within the time period of the experiment. This suggests that the dissolution of W did not have a pronounced effect on the catalytic activity when the electrode was polarized at +0.4 V. Figure 8b shows the current−time characteristics of the GC/CNT−Pt−Ru−Nafion electrode. The initial decay (up to 20 min) of the GC/CNT−Pt−Ru−Nafion electrode was more than the GC/CNT−Pt−WO_3−Nafion electrode and then gradually decreases for the next 30 min and becomes stable after 60 min. The GC/CNT/Pt−Nafion (Figure 8c) decays faster due to the poisoning, as expected, and reaches the minimum current density within 10 min.

The comparison of the CNT-based electrodes polarized at +0.6 V and +0.4 V clearly suggests that the GC/CNT/Pt−WO_3 deactivates faster when the electrode is polarized at +0.6 V. The GC/CNT/Pt−WO_3−Nafion electrode stability is poor compared to the GC/CNT−Pt−Ru−Nafion at +0.6 V. However, it not only showed initial higher activity but also was comparatively more stable than the GC/CNT/Pt−Ru−Nafion electrode when polarized at +0.4 V. This suggests that not only the utilization of catalytic particles is increased but also the stability.

TABLE 2: Evaluation of Stability of Methanol Oxidation Activity of CNT-Based Materials

		activity[a]					
		polarization at +0.6 V		polarization at +0.4 V		activ (%)	activ (%)
S.No	electrode	init (I) ($mAcm^{-2}$)	final (I) ($mAcm^{-2}$)	init (I) ($mAcm^{-2}$)	final (I) ($mAcm^{-2}$)	decr after 2 h +0.6 V	decr after 2 h +0.4 V
1	GC/CNT/Pt−WO_3−Naf	64.3	28.5	41.4	27.1	55.6	34.0
2	GC/CNT/Pt−Ru−Naf	52.8	28.5	35.7	17.8	46.1	50.0
3	GC/CNT/Pt−Naf	24.3	7.1	14.3	3.6	70.0	74.8

[a] Evaluated in 1 M H_2SO_4/1 M CH_3OH for 2 h.

The values of initial and the final current densities with the percentage decrease of activity of the electrodes polarized at +0.6 V and at + 0.4 V for 2 h are tabulated in Table 2. The Pt content used in the chronoamperometric experment was the same as that used in the cyclic voltammetric study. Because the chronoamperometric experiments were performed with only one Pt loading, the currents were normalized to the electrode geometric area.

4. Conclusions

The template-aided synthesis of carbon nanotubes using polyphenyl acetylene precursor yielded well-aligned, cylindrical, monodisperse carbon nanotubes. The higher electrochemical response of the carbon nanotube is correlated to the higher available electroactive surface area (as evaluated from the cyclic voltammetry). The open end of the carbon nanotube (as revealed from HR-TEM) has been effectively utilized to load the catalytic nanoparticles. The catalytic nanoparticles are effctively dispersed inside the tube with particle sizes of around 1.2, 1.6, and 10 nm for Pt, Pt−Ru, and Pt−WO_3, respectively. The X-ray photoelectron spectra showed the presence of Pt and Ru in the metallic state and W in +VI oxidation state. The higher activity of GC/CNT−Pt−WO_3−Nafion (as evaluated from cyclic voltammetry) compared to GC/CNT/Pt−Ru−Nafion and GC/CNT/Pt−Nafion suggests the better utilization of the catalytic particles. The stability of the electrode for methanol oxidation polarized at +0.6 V follows the order GC/CNT/Pt−Ru−Nafion ≫ GC/CNT/Pt−WO_3 > GC/CNT/Pt−Nafion, and for the electrodes polarized at +0.4 V, the order is GC/CNT/Pt−WO_3−Nafion > GC/CNT/Pt−Nafion. The differences in the stability possibly suggest the better tolerance of the adsorbed species of methanol oxidation for the GC/CNT/Pt−WO_3−Nafion electrode (when it is polarized at +0.4 V).

Acknowledgment. The authors sincerely thank Prof. Michael Graetzel, the Head and Director of ICMB, Laboratory of Photonics and Interfaces, for providing the laboratory facilities to carry out this work at the Swiss Federal Institute of Technology (EPFL), Switzerland. We thank Dr. A. J. McEvoy, of the same lab, for the fruitful discussions we had with him over this work. We also thank the Centre Interdisciplinaire de Microscopie Electronique (CIME) at EPFL for providing us with the Electron Microscopes.

References and Notes

(1) Rodriguez, N. M.; Kim, M. S.; Baker, R. T. K. *J. Phys. Chem.* **1994**, *98*, 13108.
(2) Che, G.; Lakshmi, B. B.; Fisher, E. R.; Martin, C. R. *Nature* **1998**, *393*, 346.
(3) Che, G.; Lakshmi, B. B.; Martin, C. R.; Fisher, E. R. *Langmuir* **1999**, *15*, 750.
(4) Iijima, S. *Nature* **1991**, *354*, 56.
(5) Che, G.; Lakshmi, B. B.; Martin, C. R.; Fisher, E. R. *Chem. Mater*. **1998**, *10*, 260.
(6) Gao, X. P.; Qin, X.; Wu, F.; Liu, H.; Lan, Y.; Fan, S. S.; Yuan, H. T.; Song, D. Y.; Shen, P. W. *Chem. Phys. Lett*. **2000**, *327*, 271.
(7) Hernadi, K.; Fonseca, A.; Nagy, J. B.; Bernaerts, D.; Riga, J.; Lucas, A. *Synth. Met.* **1996**, *77*, 31.
(8) Kyotani, T.; Tsai, l. F.; Tomita, A. *Chem. Mater*. **1995**, *7*, 1427.
(9) Han, T. C.; Fouseca, A.; Nagy, J. B.; Bernaerts, D.; Riga, J.; Lucas, A. *J. Chem. Soc. Chem. Commun.* **1989**, *88* 203.
(10) Kroke, E.; Schwarz, M.; Buschmann, V.; Miche, G.; Fuess, H.; Riedel, R. *Adv. Mater.* **1999**, *11*, 158.
(11) Rajesh, B.; Ravindranathan Thampi, K.; Bonard, J. M.; Viswanathan, B. *J. Mater. Chem.* **2000**, *10*, 1757.
(12) Rajesh, B.; Ravindranathan Thampi, K.; Bonard, J. M.; Viswanathan, B. *Eurasian Chem.-Technol. J.* **2001**, *3*, 11.
(13) Witham, C. K.; Chun, W.; Valdez, T. I.; Narayanan, S. R. *Electrochem. Solid-State Lett.* **2000**, *3*, 497.
(14) Parsons, R.; VanderNoot, T. *J. Electroanal. Chem.* **1988**, *257*, 1.
(15) Watanabe, M.; Motoo, S. *J. Electroanal. Chem.* **1975**, *60*, 267.
(16) Baldauf, M.; Preidel, W. *J. Appl. Electrochem.* **2001**, *31*, 781.
(17) Li, W. S.; Tian, L. P.; Huang, Q. M.; Li, H.; Chen, H. Y.; Lian, X. P. *J. Power Sources* **2002**, *104*, 281−288.
(18) Lamy, C.; Belgsir, E. M.; Leger, J. M. *J. Appl. Electrochem.* **2001**, *31*, 799.
(19) Shen, P. K.; Tseung, A. C. C. *J. Electrochem. Soc.* **1994**, *141*, 3083.
(20) Shen, P. K.; Chen, K. Y.; Tseung, A. C. C. *J. Chem. Soc., Faraday Trans.* **1994**, *90*, 3089.
(21) Shukla, A. K.; Ravikumar, M. K.; Roy, A.; Barman, S. R.; Sarma, D. D.; Arico, A. S.; Antonucci, V.; Piono, L.; Giordano, N. *J. Electrochem. Soc.* **1994**, *141*, 1517.
(22) Zhang, H.; Wang, Y.; Fachini, E. R.; Cabrera, C. R. *Electrochem. Solid-State Lett.* **1999**, *2*, 437.
(23) Bessel, C. A.; Laubernds, K.; Rodriguez, N. M.; Baker, R. T. K. *J. Phys. Chem.* **2001**, *105*, 1115.
(24) Rajesh, B.; Karthik, V.; Karthikeyan, S.; Ravindranathan Thampi, K.; Bonard, J. M.; Viswanathan, B. *Prepr. Symp. Am. Chem. Soc. Div. Fuel. Chem.* **2001**, *46*, 452.
(25) Rajesh, B.; Karthik, V.; Karthikeyan, S.; Ravindranathan Thampi, K.; Bonard, J. M.; Viswanathan, B. *Fuel* **2002**, *81*, 2177.
(26) Gita, B.; Sundararajan, G. *Polym. Prepr. (Am. Chem. Soc. Div. Polym. Chem.)* **1994**, *35*, 729.
(27) Kinoshita, K. In *Carbon-Electrochemical and Physicochemical Properties*; John Wiley and Sons: New Jersey, 1988.
(28) Bard, A. J.; Faulkner, L. R. In *Electrochemical Methods-Fundamentals and Applications*; John Wiley and Sons: New York, 2000.
(29) Figlarz, M. *Prog. Solid-State Chem.* **1989**, *19*, 1.